Di-jet cross section in photoproduction and gluon density in the photon

B. Andrieu[a] (H1 collaboration)

[a]L.P.N.H.E., Ecole Polytechnique, CNRS-IN2P3, Palaiseau, 91128 Palaiseau Cedex, France

We report on a new measurement of di-jet cross section in photoproduction, using an integrated luminosity of $\mathcal{L} \simeq 7.2$ pb^{-1} taken with the H1 detector at HERA. A leading order effective parton density of the photon is deduced, which extends down to small parton fractional energies of $x_\gamma = 0.04$. This allows a measurement, in a largely unexplored kinematic domain, of the gluon density in the photon which is compared to QCD-inspired models and to a recent H1 measurement using charged tracks.

1. INTRODUCTION

1.1. Physics motivation

In photoproduction at high p_T as observed in HERA, the photon is not only an elementary particle which interacts through QED couplings to quarks and leptons in so-called direct processes (Fig. 1a). Due to quantum fluctuations into either a vector meson carrying the same quantum numbers, or a quark-antiquark pair, the photon also acquires a hadronic resolved component which can be described by parton density functions (p.d.f.) as for normal hadrons. This distinction between direct and resolved is of course only meaningful in Leading Order (LO) QCD. The resolved photoproduction (Fig. 1b) cross section can be expressed as a sum over all parton-parton combinations of convolution products between both p.d.f of the proton and the photon, and the parton-parton cross section. Each p.d.f depends on two variables : the factorization scale, generally p_T of the outgoing parton, and the fraction x of the momentum of the parent particle carried by the incoming parton. P.d.f. of the proton are well-known from F_2 measurements[1].

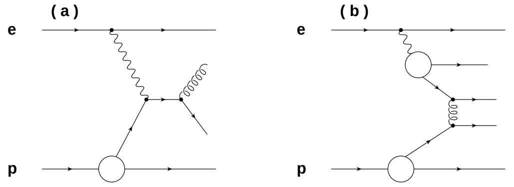

Figure 1. Examples of direct (a) and resolved (b) photoproduction diagrams.

In e^+e^- experiments, F_2^γ measurements allow to constrain the quark component of the photon[2], but up to now didn't give much information on its gluon component. In HERA, where gluons in the photon can be probed by partons from the proton, we thus have a unique possibility of constraining the gluon component of the photon.

1.2. Experimental methods

In the LO QCD picture, the parton-parton scattering processes represented in Figure 1 appear in the detector as events with two high p_T jets, which generally include also high p_T particles, sometimes accompanied by soft underlying event from remnants of the proton and the photon. The fraction x_γ of the momentum of the photon carried by the interacting parton can then be reconstructed from the two hardest jets in the event as :

$$x_\gamma^{jets} = \frac{\sum_{jet}(E - p_z)}{2E_\gamma} = \frac{\sum_{jet} E_T e^{-\eta}}{2yE_e} \qquad (1)$$

where $\eta = -\ln\tan(\theta/2)$ is the pseudo-rapidity (θ is the polar angle with respect to the proton beam direction), E_e the electrom beam energy, and $y = E_\gamma/E_e$. An event-by-event reconstruction of x_γ is then possible, but this method suffers from problems associated with jet energy measurement : the hadronic energy scale uncertainty, and the possible contamination of the soft underlying event. Since the jet cross sections are steeply falling as a function of E_T (the inclusive jet photoproduction cross section goes like $(E_T)^{-n}$, with $n \sim 6$[3]), even a small systematic

shift of E_T can induce a big error on x_γ cross section. An unfolding of x_γ cross sections at the parton level is thus necessary to suppress both these detector and physics effects in order to study the parton content of the photon.
On the other hand, high p_T charged tracks do not allow to reconstruct x_γ directly, since, for an outgoing parton with a given p_T, the number and p_T distribution of the corresponding charged tracks may vary much from event to event. A statistical correlation is however seen, which allows unfolding of x_γ from charged particle cross sections. Since high p_T charged tracks sign unambiguously the fragmentation of higher p_T partons, the contamination of soft processes can be completely suppressed. However new uncertainties appear from the fragmentation functions, which are only known experimentally, and from the measurement of charged tracks parameters.
Two methods are available to measure x_γ cross sections in photoproduction with completely different systematic errors. In both of them, but for different reasons, the parton level cross sections need to be unfolded of physics and detector effects. The comparison of these two independent measurements will thus allow to gain new information on the structure of the photon.

2. DETECTOR DESCRIPTION

A complete description of the H1 detector can be found elsewhere[4]. Here only the components used in this analysis will be described.
The central tracking system consists of several detectors mounted concentrically around the beam line : two proportional chambers are used for triggering purposes, two z-drift chambers give a precise measurement of the z coordinate along the beam axis, and two cylindrical drift chambers yield particle charge and momentum from the track curvature in the plane transverse to the beam. In the range $20^o < \theta < 160^o$ the resolution on θ is 2 mrad, and the transverse momentum resolution is $\sigma(p_T)/p_T \sim 0.6\%.p_T$ (GeV/c) for $p_T > 2$ GeV/c. In the forward direction (i.e. for $7^o < \theta < 25^o$) the central tracking system is complemented by a forward tracking system. The tracking system is also used in jet analysis to improve the hadronic energy measurement.
Surrounding the tracking system is the liquid argon (LAr) calorimeter. It is composed of an inner electromagnetic part of 20 to 30 radiation lengths deep, with lead as an absorber, and an outer hadronic part with steel as an absorber. The total depth seen by particles coming from the interaction vertex varies between 4.5 and 8 interaction lengths. The LAr calorimeter can measure the energy of particles in the range $4^o < \theta < 153^o$ with a resolution of approximately 12 $\%/\sqrt{E}$ (E in GeV) for electrons and photons, and 50 $\%/\sqrt{E}$ (E in GeV) for hadrons.
The calorimeter cryostat is surrounded by a superconducting solenoid which produces a magnetic field along the beam line of 1.15 T.
The electron tagger, which is part of the luminosity system, is a TlCl/TlBr crystal Cerenkov calorimeter located 33 m from the interaction point in the electron direction. By measuring electrons scattered at small angles with an energy resolution of 10 $\%/\sqrt{E}$ (E in GeV), it allows to tag photoproduction events in the maximal y range $0.3 < y < 0.7$.

3. DI-JET CROSS SECTION

3.1. Data selection

The data sample corresponds to a luminosity of $\mathcal{L} \simeq 7.2$ pb^{-1} collected in 1996 at HERA, where positrons of 27.5 GeV collided with protons of 820 GeV. Using the electron tagger, photoproduction events were selected in the range $0.5 < y < 0.7$, and $Q^2 < 10^{-2}$ GeV^2. Jets were then reconstructed by running the CDF cone algorithm[5], with a cone radius of 0.7, on objects combining energy clusters from the calorimeter and charged tracks from the tracking system.
In order to reduce the influence of the soft processes, a so-called pedestal energy was estimated by averaging energy outside jet in the band $-0.7 < \Delta\eta < 0.7$, $-\pi < \Delta\phi < \pi$. This pedestal energy and its dependence on η were reasonably reproduced by Monte-Carlo, which made its subtraction from the jet energy measured inside the cone reliable. After pedestal subtraction, two jets were required with $E_T > 6$ GeV fully contained in the LAr calorimeter ($-0.5 < \eta < 2.5$). The value

of 6 GeV is a compromise between the aim to go to as low E_T as possible, in order to reach low x_γ, and the need to stay in a region where perturbative QCD calculation apply. The fraction of the momentum of the photon carried by the interacting parton x_γ^{jets} was then reconstructed according to equation (1). In order to improve the jet-parton correlation, two further cuts were imposed on the two hardest jets of selected events : $|\eta_{jet1} - \eta_{jet2}| < 1$ and $\eta_{jet1,2} < -0.9 - \ln(x_\gamma^{jets})$. More details on this analysis can be found in [6].

3.2. Monte-Carlo

For correction of the data, and comparison to measured jet cross sections, the two event generators PYTHIA[7] 5.7 and PHOJET[8] 1.06 were used. Both generators include all direct and resolved processes calculated in LO QCD, as well as initial and final state parton showers in order to simulate higher orders perturbative effects. In both cases also, GRV-LO parameterizations for the parton distributions of the photon[9] and the proton[10] were used, and hadronization was modelled with the LUND string fragmentation scheme as implemented in JETSET[11] 7.4. The main difference between both generators stays in the way soft processes are treated. In PYTHIA, multiple parton interactions are generated in addition to the primary parton-parton scattering, which are calculated as LO QCD processes between partons from the photon and parton remnants.On the other hand, PHOJET, which is based on the two-component Dual Parton Model[12], incorporates very detailed simulations of both multiple soft and hard parton interactions on the basis of a unitarization scheme[13]. Two samples of Monte-Carlo events, one for each generator, equivalent to a luminosity of $\mathcal{L} \sim 13$ pb^{-1} were generated, passed through H1 detailed simulation program, and finally submitted to the same reconstruction and selection chain as the data.

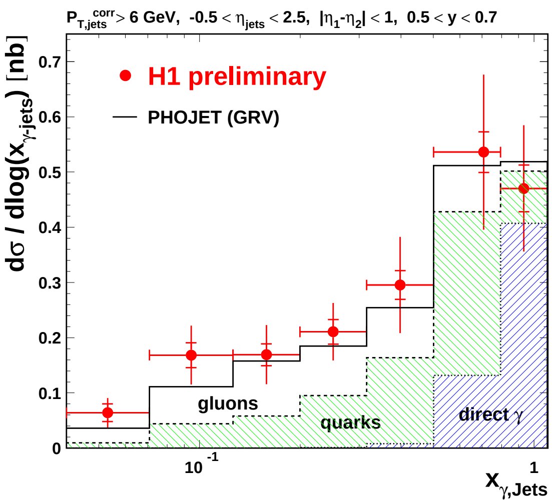

Figure 2. Di-jet x_γ cross section unfolded at the hadron level

3.3. Hadron level cross sections

In order to correct data for detector effects implying x_γ migrations, and to allow direct comparisons with Monte-Carlo models or even QCD calculations, an unfolding program[14] was used. Using Monte-Carlo "data" , the unfolded $x_{\gamma,had}$ distribution at the hadron level was shown to have good correlations with $x_{\gamma,det}$ at the detector level, down to $x_\gamma = 0.04$. Several tests of the stability of the method were also performed such as unfolding data starting from a flat x_γ input, from a different photon p.d.f. LAC1[15], or using the two different models PYTHIA and PHOJET to estimate detector corrections. A systematic error always lower than 10 % was attached to each check. Other systematic errors come from the e-tagger acceptance, the trigger efficiency, the luminosity measurement, the most important one being due to the hadronic energy scale, whose uncertainty of $\pm 4\%$ contributes to the systematic error on x_γ cross section between 10 % to 30 % in the lowest x_γ bin. The preliminary result on x_γ cross section unfolded at the hadron-level is presented in Fig. 2, together with PHOJET prediction and the contributions to PHOJET calculation from different processes. The direct part dominates at high x_γ, while the resolved part initiated by a quark and a gluon in the photon dominate at intermediate and low x_γ respectively. The PHOJET prediction agrees well with data.

3.4. Effective parton distributions

The resolved part of the ep cross section for producing two partons ab at a given p_T can be calculated in LO QCD as :

$$\frac{\mathrm{d}^4\sigma_{ab}}{\mathrm{d}y\ \mathrm{d}x_\gamma \mathrm{d}x_p \mathrm{dcos}\theta^*} = \frac{1}{32\pi s_{ep}} \frac{f_{\gamma/e}(y)}{y} \times$$
$$\sum_{ij} \frac{f_{i/\gamma}(x_\gamma, p_T^2)}{x_\gamma} \frac{f_{j/p}(x_p, p_T^2)}{x_p} |M_{ij\to ab}(\cos\theta^*)|^2 \quad (2)$$

where s_{ep} is the squared ep center-of-mass energy, y, x_γ, x_p are the fraction of the momentum of the electron, photon, proton, taken by the photon, parton i and parton j respectively, $f_{\gamma/e}(y)$ is the photon flux inside the electron, $f_{i(j)/\gamma(p)}$ are the p.d.f of parton $i(j)$ inside the photon (proton), and $M_{ij\to ab}(\cos\theta^*)$ is the QCD matrix element of the parton-parton process $ij \to ab$. The parton transverse momentum p_T is taken as the scale of the process. The method followed is detailed in [16] and is based on the approximation procedure developed in [17]. In LO QCD, the resolved part of the observed di-jet cross section is the sum over all ab outgoing partons of the cross section expressed in formula (2). The approximation exploits the observation that in this double sum over ij and ab, three generic processes dominate, namely $qq' \to qq'$, $qg \to qg$, and $gg \to gg$, which have similar angular distributions and differ only in rate by the ratio of colour factors $C_A/C_F = 9/4$. Defining effective parton density functions for the photon and the proton as :

$$\tilde{f}_k(x_k, p_T^2) \equiv \sum_{n_f}(f_{q/k}(x_k, p_T^2) + f_{\overline{q}/k}(x_k, p_T^2))+$$
$$\frac{9}{4} f_{g/k}(x_k, p_T^2) \quad (3)$$

where $k = \gamma, p$ and assuming that, except for the colour factor, the three dominant processes use only one Single Effective Subprocess matrix element M_{SES}, the resolved part of the di-jet cross section can be approximated by :

$$\sum_{ab} \frac{\mathrm{d}^4\sigma_{ab}}{\mathrm{d}y\ \mathrm{d}x_\gamma \mathrm{d}x_p \mathrm{dcos}\theta^*} \approx \frac{1}{32\pi s_{ep}} \frac{f_{\gamma/e}(y)}{y} \times$$
$$\frac{\tilde{f}_\gamma(x_\gamma, p_T^2)}{x_\gamma} \frac{\tilde{f}_p(x_p, p_T^2)}{x_p} |M_{SES}(\cos\theta^*)|^2 \quad (4)$$

The effective parton distribution of the proton being known, an effective parton distribution of the photon can now be extracted from di-jet x_γ cross section unfolded at the parton level using the same procedure as in 3.3. Again a good correlation was observed between $x_{\gamma,det}$ at the detector level and $x_{\gamma,parton}$, the "true" x_γ used in the Monte-Carlo generation. Same tests of the unfolding procedure as for the extraction to the hadron level were done, which gave same systematic errors but one : different results of unfolding were obtained when using the two Monte-Carlo samples, due to the different treatment of the soft processes. This is illustrated in Fig. 3, where both effective parton distributions extracted after unfolding to the parton level using the two different Monte-Carlo are presented. Without a clear indication of which soft processes simulation to favour, the mean value of both results is taken as preliminary measurement, and an additional systematic error, which goes from 5% to 25%, is included to take into account this Monte-Carlo dependency. On the same figure are also shown two effective parton densities of the photon calculated from the parameterizations GRV and LAC1 at a scale of 74 GeV^2, which was estimated, given the experimental selection, to be the mean scale of the hard parton-parton process in Monte-Carlo

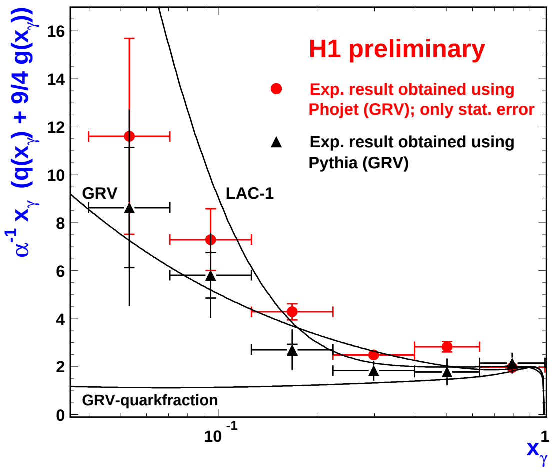

Figure 3. Effective parton distribution of the photon, after unfolding of x_γ cross section at the parton level with two different Monte-Carlo models.

events. GRV is in agreement with the data, given the large error bars, while the fast rise of LAC1 towards low x_γ is already excluded.

4. CHARGED PARTICLE CROSS SECTIONS

4.1. Data selection

The data sample corresponds to a luminosity of $\mathcal{L} \simeq 1.3$ pb^{-1} collected in 1994 at HERA, where positrons of 27.5 GeV collided with protons of 820 GeV. Using the electron tagger, photoproduction events were selected in the range $0.3 < y < 0.7$, and $Q^2 < 10^{-2}$ GeV^2. The essential requirement was a well measured charged track in the central region $|\eta| < 1$ with $p_T > 2$ GeV/c. All known detector effects were corrected for in order to produce cross sections at the hadron level, directly comparable to QCD calculations or models. A detailed description of the selection and correction procedure can be found in [18].

4.2. Monte-Carlo and NLO calculation

In addition to the two Monte-Carlo programs already used for the di-jet analysis, a program with a different hadronization scheme, HERWIG[19], was also used to study the dependence of the measurement on the fragmentation model. A complete NLO QCD calculation[20] was also compared to data. It used the NLO GRV p.d.f. for the photon, and the NLO BKK[21] fragmentation functions. In this calculation, the renormalization, factorization, and hadronization scales were all set to the same value ξp_T^2, with ξ varying between 1/2 and 2, in order to estimate the uncertainty due to the choice of the scale.

4.3. Hadron level cross sections

The γp inclusive charged particle cross section is presented in Fig. 4a and fitted to a QCD inspired power-law function of the form $A(1 + p_T/p_{T0})^{-n}$. Since the measurement starts at $p_T > 2$ GeV/c, the fit is not sensitive to the small value of p_{T0}, which is then fixed to the value 0.63, as found in [23]. The fit gives $A = 5.44 \pm 0.66$ mb and $n = 7.03 \pm 0.21$ and reproduces data well over the whole p_T range. It is presented in Fig. 4a, and compared with similar fits in $p\overline{p}$ experiments UA1[24] and CDF[25] at various c.m.s energies, scaled by the factors indicated on the figure, which essentially normalize all data to the γp cross section at $p_T = 2$ GeV/c. The hardness of the γp spectrum is clearly larger than in $p\overline{p}$ at similar c.m.s. energies, and comparable to that in $p\overline{p}$ at a c.m.s. energy almost an order of magnitude higher, which can be understood as coming from extra contributions in γp compared to $p\overline{p}$, namely the direct and pointlike resolved (or anomalous) component of the photon. The same distribution divided by the NLO QCD calculation of [20] with scale p_T^2 is shown in Fig. 4b. The shaded area shows the effect of varying the scale in the calculation between $0.5\,p_T^2$ and $2\,p_T^2$. The agreement between data and calcu-

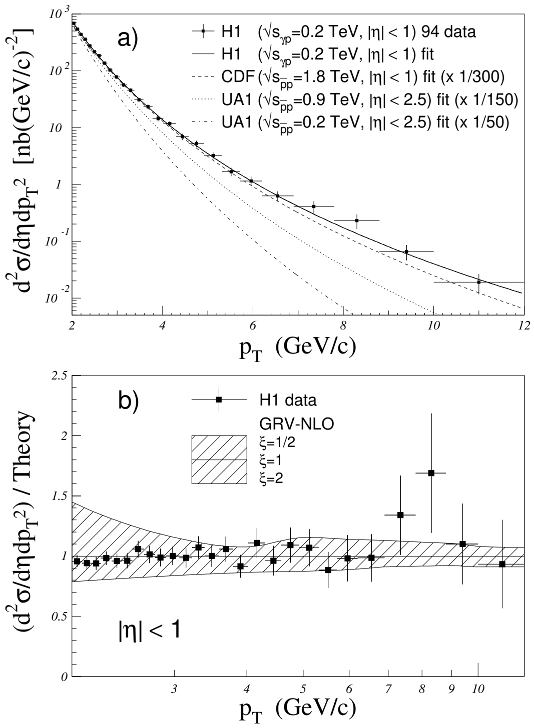

Figure 4. (a) Inclusive charged particle γp cross section and comparison of power-law fits of the same distribution in different experiments. (b) Same distribution divided by NLO QCD calculation, with all scales set to p_T^2. The shaded area shows the effect on the calculation of a variation of the scale ξp_T^2 between $\xi = 1/2$ to 2.

lation is good, unfortunately the calculation has very big uncertainties at low p_T where data are the most precise, while at high p_T where the scale uncertainties are much reduced, data points have big statistical and systematic errors.

4.4. x_γ distributions

In order to measure x_γ cross sections from charged tracks, an unfolding procedure using Monte-Carlo models had to be used. A further cut was applied on data, keeping only events with at least a track of $p_T > 2.6$ GeV/c, in order to suppress possible contamination from soft processes. This cut also helped in being not too close to the $\widehat{p}_T$ cut of 2 GeV used in PYTHIA.

For selected events, an empirical x_γ, using only information from charged tracks, was built according to the following formula :

$$x_\gamma^{rec} = \frac{\Sigma p_T e^{-\eta}}{y E_e} \tag{5}$$

where the sum is over all tracks with $p_T > 2$ GeV/c. It was shown on Monte-carlo events that this variable has good correlation with x_γ at the parton level, thus making possible to unfold x_γ from the data. The unfolding procedure of [26] was used, following the analysis as detailed in [22]. The stability of the procedure was controlled by unfolding data with different input p.d.f. (GRV vs LAC1), and different fragmentation models (PYTHIA vs HERWIG). The difference between results obtained with these different Monte-Carlo inputs of the unfolding was taken as an additional systematic error of 20 %, which, apart from the experimental errors on the measurement itself, was the most important contribution to the total systematic error.

5. Gluon density

Finally the gluon density of the real photon is extracted for both methods. For di-jet the GRV quark density in the photon is simply subtracted from the measured effective parton density of the photon. In the charged track analysis, the contribution of processes in which quarks are resolved in the photon, is first subtracted from the observed x_γ thus giving an estimation of the gluon initiated processes. This measured gluon x_γ distribution is then compared to the equivalent distribution for Monte-Carlo. The resulting weight factors obtained by the ratio of both distributions are finally applied bin-by-bin to the input p.d.f. used in Monte-Carlo to give the measured gluon density. The gluon densities obtained by both methods are presented in Fig. 5 and compared to the predictions of GRV and LAC1 at a mean scale of $< p_T^2 >= 74$ GeV^2. It should be noted that the average transverse momentum squared of the hard partonic scattering for the data sample used in the charged track analysis was estimated from Monte-Carlo to be $< p_T^2 >= 38$ GeV^2/c^2, but the difference between the predictions of the p.d.f. due to this scale difference is of the order of 5 % at maximum in the lowest x_γ bin. Given the limited precision on measured gluon density, the agreement is very good between both methods. The rise of gluon density with decreasing x_γ is clearly established. GRV is a bit below the data points at low x_γ, but still well within the error bars. A fast rise of the gluon density, as present in LAC1, is on the contrary excluded.

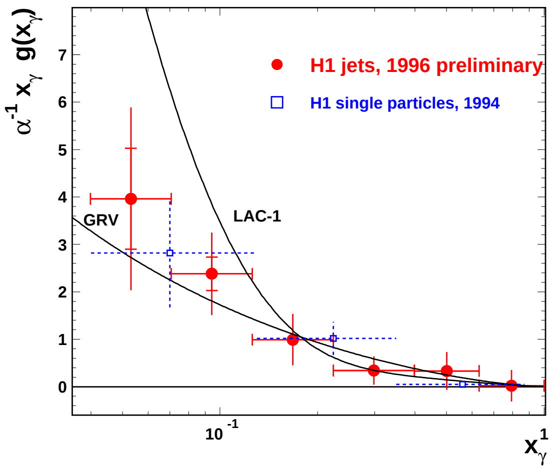

Figure 5. Gluon density of the photon, obtained using either di-jet or charged particle cross sections, and comparison with two parameterizations of the photon structure.

6. CONCLUSION

A new preliminary measurement of the di-jet cross section in tagged photoproduction at HERA has been presented. The pedestal energy was subtracted from the jet core in order to reduce the influence of the soft processes in the measurement. After unfolding to the parton level, a leading-order effective parton density of the photon was extracted, which extends down to $x_\gamma = 0.04$. Results on charged particle cross sections were also presented which show a good agreement with a NLO QCD calculation. The x_γ distribution was unfolded from the data using for the first time high p_T charged tracks. Gluon density could then be extracted in both methods. There is a good consistency between both measurements, which can be considered largely independent given the different techniques used in event selection and result extraction, and consequently the different systematic errors attached to these results. The gluon density is shown to rise towards low x_γ. A moderate rise as predicted by GRV p.d.f. is in agreement with the data, while a fast rise of the gluon density of the photon as predicted by LAC1 p.d.f. is clearly excluded.

Acknowledgements

It is a pleasure to thank S. Söldner-Rembold and the organizing commitee for this fruitful meeting. I would also like to thank O. Kaufmann for his help in preparing the presentation.

REFERENCES

1. U. Bassler et al., Int. Workshop on Deep Inelastic Scattering and QCD (DIS99), Zeuthen (Germany) 19-23 April 1999.
2. R. Nisius, these proceedings.
3. ZEUS Coll., M. Derrick et al., *Phys. Lett.* B342 (1995) 417.
4. H1 Coll., I. Abt et al., *Nucl. Instrum. Methods* A386 (1997) 310 and 348.
5. J. Huth et al., Proceedings of the 1990 DPF Summer Study on High Energy Physics, Snowmass (Colorado) ed. E.L. Berger, World Scientific (1992) 134 ; CDF Coll. F. Abe et al., *Phys. Rev.* D45 (1992) 1448.
6. O. Kaufmann, PhD Thesis, Heidelberg (1998).
7. T. Sjöstrand, CERN-TH-6488 (1992), *Comput. Phys. Commun.* 82 (1994) 74.
8. R. Engel, *Z. Phys.* C66 (1995) 203 ; R. Engel and J. Ranft, *Phys. Rev.* D54 (1996) 4244.
9. M.Glück, E. Reya and A. Vogt, *Phys. Rev.* D46 (1992) 1973.
10. M.Glück, E. Reya and A. Vogt, *Z. Phys.* C53 (1992) 127..
11. T. Sjöstrand, M. Bengtsson, *Comput. Phys. Commun.* 43 (1987) 367.
12. A. Capella et al., *Phys. Rep.* 236 (1994) 225.
13. A. Capella et al., *Phys. Rev. Lett.* 58 (1987) 2015.
14. G. D'Agostini, *Nucl. Instrum. Methods* A362 (1995) 487.
15. H. Abramowicz, K. Charchula, A. Levy, *Phys. Lett.* B269 (1991) 458.
16. H1 Coll., C. Adloff et al., *Eur. Phys. J.* C1 (1998) 97.
17. B.V. Combridge and C.J. Maxwell, *Nucl. Phys.* B239 (1984) 429.
18. H1 Coll., C. Adloff et al., DESY 98-148, hep-ex/9810020, submitted to *Eur. Phys. J.* C.
19. G. Marchesini et al., *Comput. Phys. Commun.* 67 (1992) 465.
20. F.M. Borzumati, B.A. Kniehl and G. Kramer, *Z. Phys.* C59 (1993) 341 ; B.A. Kniehl and G. Kramer, *Z. Phys.* C62 (1994) 53 ; B.A. Kniehl, hep-ph/9709261 and Proceedings of the Ringberg Workshop "New Trends in HERA Physics", Ringberg Castle (Germany) 25-30 May 1997.
21. J. Binnewies, B.A. Kniehl and G. Kramer, *Phys. Rev.* D52 (1995) 4947.
22. H1 Coll., T. Ahmed et al., *Nucl. Phys.* B445 (1995) 195.
23. H1 Coll., I. Abt et al., *Phys. Lett.* B328 (1994) 176.
24. UA1 Coll., C. Albajar et al., *Nucl. Phys.* B335 (1990) 261.
25. CDF Coll., F. Abe et al., *Phys. Rev. Lett.* 77 (1996) 438.
26. V. Blobel, DESY 84-118 and Proceedings of the CERN School of Computing, Aiguablava (Spain) CERN 1985.